2025 American Control Conference (ACC)
July 8-10, 2025. Denver, CO, USA

MIMO-decoupling to improve pressure and flow tracking in mechanical ventilation

Lars van de Kamp[1,2], Isabelle Franklin[1], Bas van Loon[1], Tom Oomen[2,3], and Nathan van de Wouw[2]

***Abstract*— Mechanical ventilators are complex mechatronic devices that are essential for patients who are unable to breathe independently. The aim of this paper is to develop a systematic control method that achieves accurate tracking of both the pressure and flow to ensure comfortable breathing for the patient. This is achieved by using a feedback design procedure technique based on static decoupling and the factorized Nyquist criterion. Furthermore, switching controllers are introduced that allow for improved baseflow tracking performance. The presented control method is implemented in a real ventilator and it is demonstrated that the tracking performance is improved by conducting an experimental case-study.**

I. Introduction

Mechanical ventilation is crucial in Intensive Care Units (ICUs) to assist patients unable to breathe independently. The goal of mechanical ventilation is to ensure adequate oxygenation and carbon dioxide elimination for a large variety of patients [1]. In 2005 alone, over 790.000 patients were reliant on mechanical ventilation to survive [2]. Therefore, improving mechanical ventilation improves treatment for a large population worldwide, especially during the flu-season or a world wide pandemic, such as the COVID-19 pandemic in recent years.

In pressure-controlled ventilation, the ventilator aims to track a pressure profile at the patient's airway to ensure sufficient airflow in and out of the lungs [3]. In addition, the ventilator aims to track a baseflow target, which is a constant flow target that ensures that the breathing hoses contain fresh air, i.e., residues of CO_2-rich exhaled air are washed out. A schematic representation of the system, including breathing hose and patient, is depicted in Figure 1. In this figure, seen from a control perspective, the system tracks two references, i.e., the pressure target and the baseflow target. The measured output that should track these references are the output pressure (p_{out}), output flow (Q_{out}), and expiration flow (Q_{exp})[1]. During an inspiration, a part of the output flow is used to build up pressure in the lungs, and a part is being used as a baseflow to flush the hose. In order to regulate these outputs, there are two actuators to be controlled, i.e., a blower and an expiration valve. A change in the actuator signal(s) for either the blower and/or the expiration valve results in a change in both the pressure and flow outputs. Inherently, the input and outputs are coupled. Ignoring this coupling during control design leads to performance limitations and stability issues. Therefore, coupling must be taken into account during controller design.

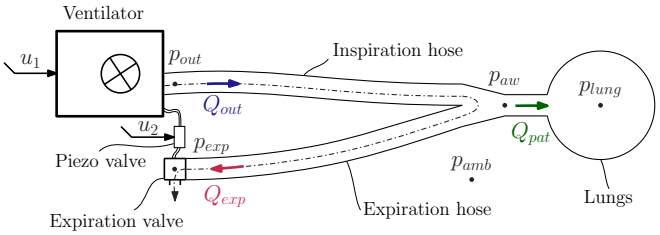

Fig. 1. Schematic overview of the ventilator and patient system, with the definition of the important pressure and flows. The inputs u_1 and u_2 of the system are, respectively, the blower revolution speed and the piezo voltage.

In Figure 2, an example of the reference trajectories for the airway pressure and baseflow are depicted together with the exemplary response of the associated pressure and flow signals. In this figure, it is clear that the output flow (Q_{out}) cannot track the baseflow reference during the whole breathing cycle; namely during an inspiration typically more output flow is required than the baseflow target in order to pressurize the lungs. Similarly the expiration flow (Q_{exp}) cannot be used to track the baseflow during expiration because of the extra air the patient exhales. Therefore, a switch between these two flow sensors is required to track the baseflow target during a full breathing cycle. Also, this switching definition of the flow tracking error challenges the controller design.

Accurate tracking of the pressure and flow references ensures sufficient fresh air delivery and improves patient comfort. According to [4], improved pressure tracking can decrease the incidence of patient-ventilator asynchrony. In [5], patient-ventilator asynchrony is associated with longer hospital stays and increased mortality rates. Furthermore, accurate pressure and flow tracking for a wide range of patients improves consistency of treatment over these different patients.

The controller design must satisfy the following requirements:

(i) The controller must simultaneously track the pressure and the baseflow references while accounting for multivariate input-output interaction.
(ii) The controller must contain a switching strategy to track the baseflow based on different flow sensors.

From a control perspective, the (unknown) patient is part of the to-be-controlled system. The challenging problem of pressure and flow tracking in presence of widely varying patients has accelerated the development of a wide range of pressure control methodologies. Methods that resulted in improved tracking performance of either pressure or flow targets are variable-gain control [4], adaptive feedback control [6], model predictive control [7], adaptive hose compensation control [8]. The tracking performance can be even further improved by leveraging the repetitive nature

[1]Demcon life sciences and health Eindhoven, Best, the Netherlands
[2]Department of Mechanical Engineering, Eindhoven University of Technology, Eindhoven, the Netherlands
[3]Delft Center for Systems and Control, Delft university of Technology, Delft, the Netherlands

[1]A detailed explanation of how these three outputs should track the two references is provided in Section II.

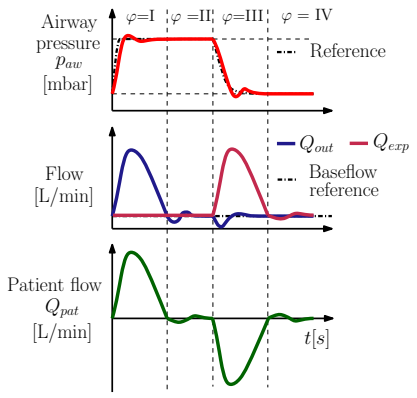

Fig. 2. Schematic overview of the ventilator and patient system, with the definition of the references and the measured pressure and flows. The locations of the pressure and flows within the system are indicated in Figure 1.

of breathing with iterative learning control [9], [10] and repetitive control [11], [12].

Although the above control techniques have substantially improved the pressure tracking performance, they do not yet satisfy both requirement (i) and (ii). The challenge of simultaneously tracking the pressure and the flow via the blower and expiration valve has not been addressed in literature. In multi-variable control, there are different solutions to cope with interaction during control design [13]. In this paper, the focus lies on decoupling control as it is an intuitive approach to deal with interaction in the system dynamics. Decoupling control helps to reduce interaction (i.e., diagonalize the system), which potentially makes it possible to design controllers for the pressure and flow loops separately. Additionally, a switch is required to track the flow target for an entire breath; also this problem has not been addressed in the literature.

The main contribution of this paper is to present an intuitive design procedure for a switching, multi-variable control strategy for mechanical ventilation that is able to cope with interaction to improve the tracking performance. The first sub-contribution is an interaction analysis of the MIMO ventilation system. The second sub-contribution is the design and implementation of a novel controller in an experimental set-up and a related performance analysis.

The paper follows the following structure. In Section II, the ventilaton system, the control goals and challenges, and the envisioned approach are presented. In Section III, the experimental set-up is introduced and the interaction in mechanical ventilation is analyzed. In Section IV, the controller concept, the decoupling procedure, and the design approach are explained. Thereafter, in Section V, the performance analysis is conducted based on an experimental case study on a mechanical ventilator. Finally, in Section VI, conclusions and recommendations are given.

II. Control Problem Formulation

A. High-level system description

Considering Figure 1, the main components of this system are the blower, the inspiration and expiration hose, the expiration valve, the piezo actuator, and the patient. A patient is characterized by the lung resistance and compliance, which influence the pressures and flow in the rest of the system. The blower and the expiration valve should jointly ensure the pressure build-up at the outlet of the blower, i.e., p_{out}, which is realized by a combination of increasing the blower speed u_1 and by increasing the piezo voltage u_2 (i.e., closing of the expiration valve). Using a model of the breathing hose, we can control p_{out} in order to achieve the desired patient airway pressure p_{aw} (defined by the clinician).

A mechanical breath can typically be subdivided into four breath phases (φ) as shown in Figure 2. The inspiration consists of phases $\varphi \in \{\text{I, II}\}$ and the expiration is covered by phases $\varphi \in \{\text{III, IV}\}$. A flow Q_{out} in the inspiration hose is caused by the pressure difference between the outlet pressure and the airway pressure of the patient. The pressure difference between the airway and lung induces the patient flow Q_{pat}, while the difference between the airway pressure and pressure located near the expiration valve (p_{exp}) induces an expiration flow Q_{exp} through the expiration hose. During all phases of the breath a baseflow Q_{bf} must be present from the output of the ventilator straight to the expiration valve to refresh the air in the hoses. As already stated in the introduction, the baseflow measurement cannot be expressed by only one measured flow variable during the whole breathing cycle, but needs to be reconstructed using both the outlet and expiration flow. Therefore, the baseflow Q_{bf} is defined as follows:

$$Q_{bf} := \begin{cases} Q_{exp} \text{ if } \varphi \in \{\text{I, II}\}, \\ Q_{out} \text{ if } \varphi \in \{\text{III, IV}\}. \end{cases} \tag{1}$$

B. Control goals and challenges

This paper considers Pressure Controlled Mandatory Ventilation (PCMV) of fully sedated patients. The goal of this system in PCMV mode is to track a preset airway pressure reference $p_{aw,\text{target}}$ given by the clinician while maintaining a constant level of baseflow $Q_{bf,\text{target}}$ during the entire breath as seen in Figure 2. The overall control goal is to minimize the tracking errors, defined by

$$\begin{aligned} e_p &:= p_{out} - p_{out,\text{target}}, \\ e_Q &:= Q_{bf} - Q_{bf,\text{target}}, \end{aligned} \tag{2}$$

where $p_{out,\text{target}}$ is derived from the airway pressure reference $p_{aw,\text{target}}$ based on model of the hose as described in [8]. In a clinical context, a sensor can only be used for either control or monitoring purposes and p_{aw} is used for monitoring purposes only. Therefore, the control goal is defined on the outlet pressure level since the outlet pressure p_{out} is a measured system output. Furthermore, note that the measured system outputs, the outlet flow Q_{out} and expiration flow Q_{exp} are both used in the definition of the baseflow Q_{bf} in (2). This induces a switch in the measured output used for feedback and hence introduces a switch in the control system and closed-loop dynamics, which challenges the control design.

Besides the switching-related challenge mentioned above, also the inherent coupling of the multivariable inputs and outputs through the system dynamics challenges the controller design. Namely, this coupling requires a control design that copes with such multivariable interaction. This interaction can result in an unstable system, or poor

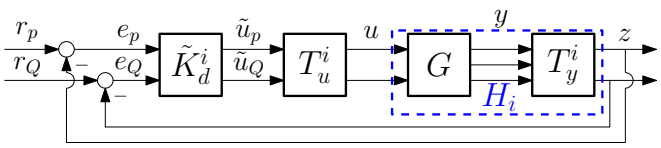

Fig. 3. Schematic overview of the proposed control scheme with $i \in \{1, 2\}$. During inspiration (phases $\varphi \in \{\text{I, II}\}$) $i = 1$ and during (phases $\varphi \in \{\text{III, IV}\}$) expiration $i = 2$.

performance, if this interaction is not taken into account in the design process.

C. System description and control approach

In this section, a high-level explanation of the control approach is presented. The goal of this control approach is to achieve good tracking performance for both the airway pressure and baseflow while keeping the controller design approach intuitive. This is achieved by designing a decentralized controller while taking interaction into account. Consider Figure 3, and let us first focus on the inputs and outputs of the plant G. There are two inputs, i.e., $u = [u_1,\ u_2]^\top$, where u_1 is the blower speed and u_2 the piezo voltage. The plant has three measured outputs, $y = [y_1,\ y_2,\ y_3]^\top$, which represent p_{out}, Q_{out} and Q_{exp}, respectively. The output selection matrix T_y^i selects the appropriate system outputs during each breathing phase such that the performance variables are defined as

$$z := \begin{cases} \begin{bmatrix} p_{out} \\ Q_{bf} \end{bmatrix} = T_y^1 y = \begin{bmatrix} 1 & 0 & 0 \\ 0 & 0 & 1 \end{bmatrix} y & \text{if } \varphi \in \{\text{I, II}\}, \\ \begin{bmatrix} p_{out} \\ Q_{bf} \end{bmatrix} = T_y^2 y = \begin{bmatrix} 1 & 0 & 0 \\ 0 & 1 & 0 \end{bmatrix} y & \text{if } \varphi \in \{\text{III, IV}\}. \end{cases} \tag{3}$$

Hence, we have a 2×2 MIMO system in which switches occur at the transitions of breathing phases (between φ =II and φ =III and between φ =IV and φ =I) at repetitive, exactly known, moments in time.

To satisfy requirements (i) and (ii), the following controller design approach is taken:

1) Design of the static decoupling matrix T_u^i, for $i = 1, 2$ (recall that $i = 1$ for $\varphi \in \{\text{I, II}\}$ and $i = 2$ for $\varphi \in \{\text{III, IV}\}$), using the interaction index to reduce interaction around the static gain region of the system.
2) Decentralized controller design of $\tilde{K}_d^{\,i}$, for $i = 1, 2$, using standard loop-shaping techniques together with the factorized Nyquist Criterion. The latter method is used to cope with residual interaction after static decoupling.

Such a decentralized (SISO) approach enables the usage of loop-shaping-based techniques [14, p. 429] for the pressure and flow loops, which makes the design approach intuitive. Note that these two steps should be executed for both the inspiration and expiration phases (i.e., for $i = 1$ during inspiration and for $i = 2$ during expiration).

III. Interaction in Mechanical Ventilation

An analysis of the interaction between the different input and outputs for mechanical ventilation is presented in this section. First, the experimental set-up is introduced. Thereafter, the Frequency Response Function (FRF) measurements, used to non-parametrically identify the dynamics, are presented together with an analysis of these dynamics. Lastly, an interaction analysis is presented.

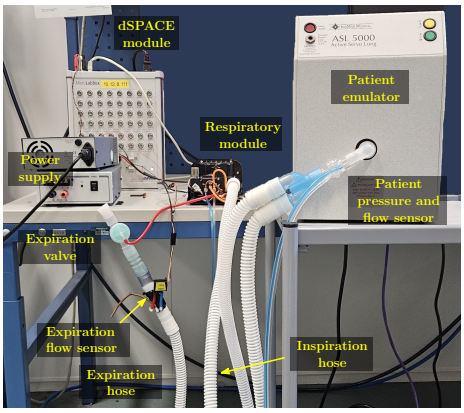

Fig. 4. Experimental setup consisting of the blower driven ventilator, ASL 5000 breathing simulator, dSpace module, hose system, expiration valve, and expiration flow sensor.

A. Experimental set-up description

The main components of the experimental setup are depicted in Figure 4. The figure shows a Macawi blower-driven mechanical ventilation module (Demcon Macawi respiratory systems, Best, The Netherlands). Furthermore, the ASL5000™ Breathing Simulator (IngMar Medical, Pittsburgh, PA) is shown in Figure 4. The breathing emulator is used to simulate a linear one-compartmental lung model as described in [15]. Additionally, a typical dual hose system used in a hospital setting is shown. At the end of the expiration hose, an expiration valve (GaleMed, Yilan, Taiwan) with an additional flow sensor is placed. The control and ventilation algorithms are implemented on a dSPACE system (dSPACE GmbH, Paderborn, Germany).

B. System identification

The system G (dynamics between inputs u and outputs y (see Figure 3) consists of the ventilator, patient, inspiration and expiration hose, piezo valve, and the expiration valve as seen in Figure 4. In this paper, we emulate a patient with a lung resistance of 50 mbar s/ml and a lung compliance of 20 ml/mbar. To identify G, FRF measurements are conducted by exciting the different inputs in u consecutively with band-pass filtered white noise (and measuring the resulting outputs in y). The excitation frequency is restricted to the 0.1 to 60 Hz range, because this is the region of interest. The magnitude plots of the frequency response functions are shown in Figure 5. The outlet pressure ($y_1 = p_{out}$) and outlet flow ($y_2 = Q_{out}$) are measured at the same location as shown in Figure 1. In general, we observe that all FRFs have a zero slope at the low-frequencies. Above 1 Hz, the patient dynamics start to play a significant role leading to a decrease in magnitude. The roll-off at higher frequencies (>10 Hz) is due to ventilator dynamics. In general, the FRFs from $u_2 = u_{piezo}$ to the outputs rolls off at a lower frequency compared to those related to the first input u_1 (blower speed). These details are important for the interaction analysis that is described in the following section.

C. Interaction

A frequency-domain interpretation of interaction, the Relative Gain Array (RGA) [16], is used for the two-sided

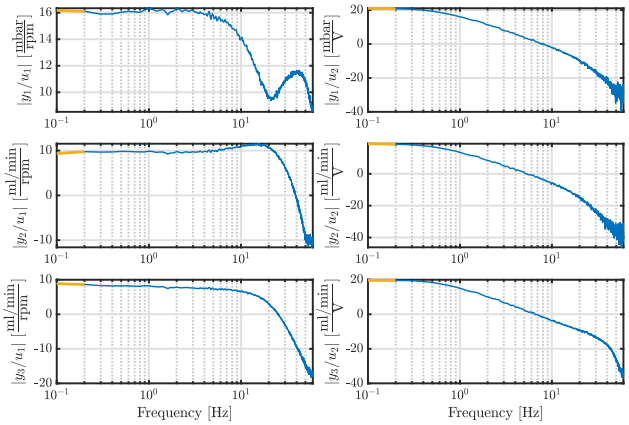

Fig. 5. Frequency response function measurements of the plant G. The highlighted orange part (—) is used for the static decoupling. The magnitude is plotted in decibels.

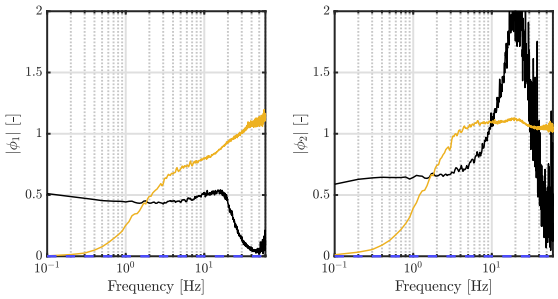

Fig. 6. Interaction index of the $\underline{H}_1(j\omega) = T_y^1 G(j\omega)$ system (—) and $H_1(j\omega) = T_y^1 G(j\omega) T_u^1$ system (—) on the left and the $\underline{H}_2(j\omega) = T_y^2 G(j\omega)$ (—) and the $H_2(j\omega) = T_y^2 G(j\omega) T_u^2$ system (—) on the right.

interaction analysis. Considering a system represented by the FRF $\underline{H}_i := T_y^i G$, see Figure 3, then the RGA is defined as

$$\Lambda_i(j\omega) := \underline{H}_i(j\omega) \odot \left(\underline{H}_i(j\omega)^{-1}\right)^\top, \quad \forall \omega \in \mathbb{R}, \tag{4}$$

where $\odot$ denotes the element-wise product. For a 2×2 system, the RGA is fully specified by the interaction index [14]:

$$\phi_i(j\omega) := \frac{\underline{H}_i^{12}(j\omega)\underline{H}_i^{21}(j\omega)}{\underline{H}_i^{11}(j\omega)\underline{H}_i^{22}(j\omega)}, \quad \forall \omega \in \mathbb{R}, \tag{5}$$

where $\underline{H}_i^{kl}$ with $k, l \in \{1, 2\}$ are the $\{k, l\}$ elements of $\underline{H}_i$. An interaction index of zero means that no interaction is present, which allows for decentralized controller design. In Figure 6, the interaction indices for both systems $\underline{H}_i$, $i = 1, 2$, are shown. For both systems, the interaction indices are not equal to zero on the displayed frequency domain, i.e., interaction is present. The interaction of the plant $\underline{H}_1$ is smaller compared to plant $\underline{H}_2$, which is pre-dominantly caused by the sensor positions. In $\underline{H}_1$, the pressure and flow are measured at a different location, namely p_{out} and Q_{exp}, while in $\underline{H}_2$, the pressure and flow are measured at the same position, namely p_{out} and Q_{out}, inherently leading to more coupling in the latter case. To justify (decentralized) SISO controller design of the diagonal elements of $\underline{H}$, the interaction index is used as a figure of merit. In the upcoming section, a decentralized controller is designed that copes with the interactions, by first introducing a static decoupling and then pursuing decentralized controller design.

IV. Decoupling-based controller design in mechanical ventilation

A control strategy that satisfies requirement (i) is presented in this section. First, static decoupling is investigated to reduce interaction. Secondly, the factorized Nyquist criterion is used as a criterion to design a decentralized controller that is robust against residual interaction.

A. Design of the static decoupling matrix

The interaction within a system can be reduced by decoupling the system dynamics. In static decoupling, a constant matrix T_u^i computes a linear transformation of the outputs of $\tilde{K}_d^i$, see Figure 3, which are subsequently used as plant inputs in order to decrease interaction by diagonalizing the plant (statically). In mechanical ventilation, accurate plants models are typically not available due to the unknown patient dynamics. This makes it challenging to consider dynamic decoupling. However, static decoupling should be possible because the patient dynamics only slightly influence the static behavior, which allows for robust design of a static decoupling matrix.

When an accurate plant model would be available, a diagonalized plant at a certain frequency could be obtained by multiplying the plant with the inverse. Plant data is complex-valued, but a decoupling matrix must be real valued in order to implement it because an actuator only allows real input values. This real-valued inverse of the frequency response data can be approximated using the ALIGN algorithm [14], leading to a static decoupling matrix

$$T_u^i := \text{ALIGN}(\overline{G}), \tag{6}$$

where $\overline{G}$ is the average frequency response data over the (low) frequency range indicated by the tick orange line in Figure 5. In this case, decoupling around the static gain results in the best improvement because it has a constant zero slope. The improved interaction indices of $H_i := T_y^i G T_u^i$ with $i \in \{1, 2\}$ are shown in Figure 6 (in orange). Due to the dynamics of the plant, i.e, different slopes because of the roll-off, it is only possible to decrease interaction locally in the (low) frequency domain. Static decoupling decreases interaction there but increases interaction above 1 Hz. Static decoupling does not decrease the two-way interaction sufficiently in the whole frequency range. Therefore, it is decided to still take the interaction into account during (robust) controller design with the help of the factorized Nyquist criterion.

B. Decentralized controller design

An intuitive controller design approach in the frequency domain is required that provides a clear guide on how to cope with residual interaction, after static decoupling, over a frequency range during decentralized design. The factorized Nyquist criterion satisfies these requirements and helps to design controllers that are robust against interaction by taking them into account during the design process. The factorized Nyquist criterion used for decentralized design is briefly described below, see also [17].

Consider a system $H(j\omega) \in \mathbb{C}^{n \times n}$ with the diagonal terms

$$\tilde{H} = \text{diag}(H^{kk}) \tag{7}$$

with $k = 1, 2$ and the normalized off-diagonal terms

$$E = (H - \tilde{H})\tilde{H}^{-1} \tag{8}$$

with $E \in \mathbb{C}^{n\times n}$. The return difference matrix is defined as

$$I + HK = I + (I + E)\tilde{H}K = (I + E\tilde{\mathcal{T}})(I + \tilde{H}K) \tag{9}$$

with $I \in \mathbb{R}^{n\times n}$ the identity matrix, controller $K \in \mathbb{C}^{n\times n}$, and

$$\tilde{\mathcal{T}} = \tilde{H}K\left(I + \tilde{H}K\right)^{-1}, \tag{10}$$

$\tilde{T} \in \mathbb{C}^{n\times n}$, which is the complementary sensitivity that would be obtained if the system was diagonal; i.e. interaction free. This results in the sensitivity function

$$(I + HK)^{-1} = \underbrace{\left(I + \tilde{H}K\right)^{-1}}_{\tilde{S}}\underbrace{\left(I + E\tilde{\mathcal{T}}\right)^{-1}}_{\text{interaction}}. \tag{11}$$

For the MIMO system to be stable, the sensitivity of the diagonal terms $\tilde{S} \in \mathbb{C}^{n\times n}$ and the interaction term in (8) must both be stable. The first term is stable by design, while a criterion for the interaction term to be stable can be derived based on the small-gain theorem [18]. Note that the interaction term consists of a part that only depends on the plant E and a part ($\tilde{\mathcal{T}}$) that consists of the diagonalized plant and controller. The interaction term is stable if

$$\rho(E(j\omega)\tilde{\mathcal{T}}(j\omega)) < 1 \;\; \forall\omega, \tag{12}$$

where ρ denotes the spectral radius. Furthermore, it holds that

$$\rho(E\tilde{\mathcal{T}}) \leq \mu_{\tilde{\mathcal{T}}}(E\tilde{\mathcal{T}}) \leq \bar{\sigma}(\tilde{\mathcal{T}})\mu_{\tilde{\mathcal{T}}}(E), \tag{13}$$

where $(j\omega)$ is omitted for clarity and $\mu_{\tilde{\mathcal{T}}}$ is the structured singular value of E with respect to the structure of $\tilde{\mathcal{T}}$, see also [14]. A controller is robust against interaction and the resulting closed loop is stable if

$$\bar{\sigma}\left(\tilde{\mathcal{T}}(j\omega)\right) < \mu^{-1}_{\tilde{\mathcal{T}}}\left(E(j\omega)\right) \;\; \forall\omega, \tag{14}$$

where we used (12) and (13). This frequency-dependent criterion can be used as a design tool for each of the SISO controllers to be robust against interaction.

Next, two pure integrator controllers

$$\tilde{K}_{d,1}(s) = \begin{bmatrix} \frac{30}{s} & 0 \\ 0 & \frac{10}{s} \end{bmatrix} \quad \text{and} \quad \tilde{K}_{d,2}(s) = \begin{bmatrix} \frac{16}{s} & 0 \\ 0 & \frac{12}{s} \end{bmatrix} \tag{15}$$

are designed to stabilize the systems H_1 and H_2, respectively. Due to the system dynamics, a controller $\tilde{K}_{d,i}$ with pure integrators already stabilizes the system and satisfies the rules of thumb for the robustness margins regarding controller design as visualized by the Nyquist plot in Figure 7. In Figure 8, it is shown that the criterion in (14) is satisfied for both H_1 and H_2.

The individual systems are now stable by design, but the closed loop of the overall system (that contains a switch) is not necessarily stable. Theoretically, Lyapunov-based results [19] can be used to proved that the closed loop of the overall system is input-to-state stable (ISS) with respect to the references r_p and r_Q. The theoretical stability analysis is omitted for the sake of brevity; hence, the switching is only experimentally verified to ensure that it indeed does not result in unstable behavior.

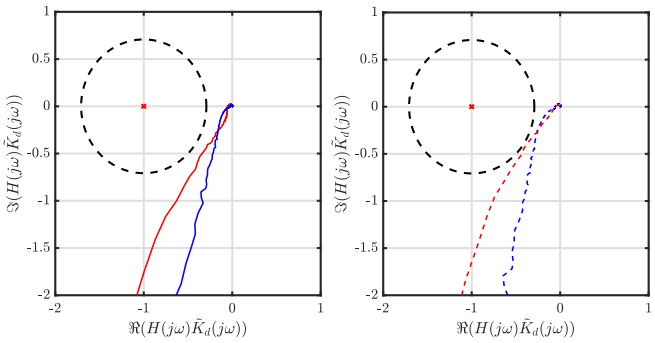

Fig. 7. Nyquist plots of the open loop SISO systems: $H_1^{11}\tilde{K}_{d,1}^{11}$ (——), $H_1^{22}\tilde{K}_{d,1}^{22}$ (——), $H_2^{11}\tilde{K}_{d,2}^{11}$ (- - -), and $H_2^{22}\tilde{K}_{d,2}^{22}$ (- - -). All individual SISO system are closed-loop stable based on the Nyquist plots. The dashed line (- - -) represents the 3 dB modulus margin threshold.

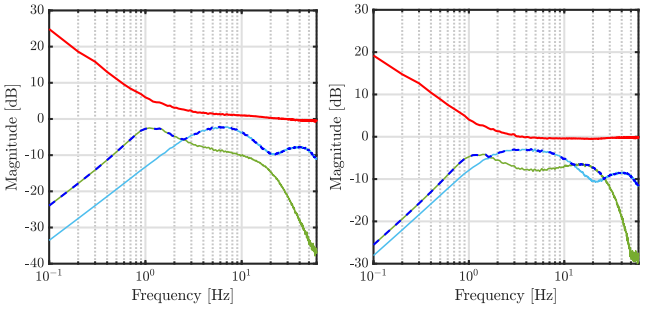

Fig. 8. Stability and robustness assessment using the factorized Nyquist criterion, with $H_1(j\omega) = T_y^1 G(j\omega)T_u^1$ system on the left and the $H_2(j\omega) = T_y^2 G(j\omega)T_u^2$ system on the right. The red line (——) represents the structured singular value of the interaction term $\mu^{-1}_{\tilde{\mathcal{T}}}(E)$ and the blue dashed line (- - -) is the maximum singular value $\bar{\sigma}(\tilde{\mathcal{T}})$, which is the maximum of the magnitude of the diagonal elements $|\tilde{\mathcal{T}}^{11}|$ (——) and $|\tilde{\mathcal{T}}^{22}|$ (——).

V. Experimental Case-Study

In the experimental case-study, a real mechanical ventilator and a lung emulator are used to analyze the tracking performance of the designed controller with the proposed methodology. For now, the focus lies on a single patient (emulated by the ASL 5000 breathing simulator, see Figure 4), where the tracking performance in the time domain is analyzed[2].

The control strategy designed in the previous section is implemented in the experimental setup of Figure 4. The results of the experiments are presented in Figure 9. The tracking performance of the designed controller is compared to the state-of-practice controller that only uses the outlet pressure p_{out} and the outlet flow Q_{out} sensors, thus making it impossible to track the baseflow during inspiration. Furthermore, the state-of-practice controller ignored interaction during design.

[2]For the sake of clarity, the control design methodology and results analysis is conducted based on a single patient. Identification of the system with different patients results in a system with uncertainty due to the different patient characteristics which are part of the plant. In that case, the uncertainty must be taken into account during control design.

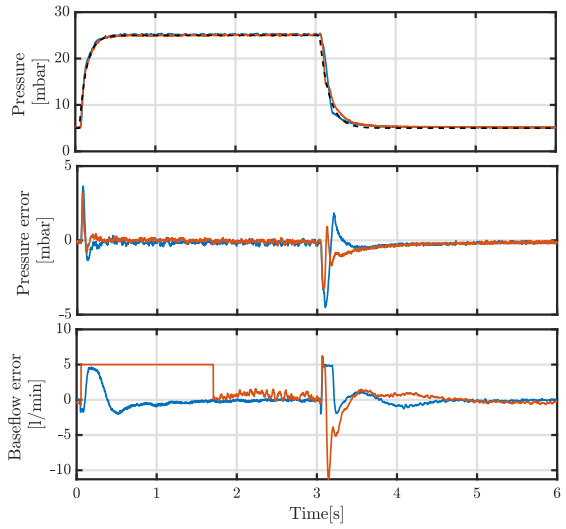

Fig. 9. Time-domain results of pressure tracking a single patient breath with the accompanied pressure and baseflow errors, where the proposed controller is displayed as (——) and the state-of-practice controller is displayed as (——). The pressure target is displayed as (- - -) in top plot.

The results of the pressure tracking of a patient breath for both control strategies are shown in top plot of Figure 9 and the tracking errors are shown in the bottom two plots. Both control strategies show accurate tracking of the pressure and flow targets. The proposed controller converges to the baseflow reference faster with more smooth inputs than the state-of-practice controller due to the proposed switching strategy. Furthermore, the state-of-practice controller fully closes the valve during the first phase of the breath because the baseflow cannot be tracked, hence introducing discontinuities in the baseflow Q_{bf}.

The pressure error during pressure build-up and decrease are slightly larger for the proposed method compared to the state-of-practice. Furthermore, the root mean square error (RMSE) of the pressure error for the state-of-practice and the decentralized controller are 0.44 and 0.58 mbar, respectively. The base flow error of the proposed method is improved compared to the state-of-practice controller. The proposed method is able to track the baseflow in the first phase of a breath and the overshoot during expiration is decreased. The total RMSE of the baseflow over a single breath decreased significantly from 2.9 l/min to 1.2 l/min by implementing the proposed controller. In general, we conclude that the tracking performance is better compared to the state-of-practice, because the additional benefits of improved flow tracking (e.g., better flushing of the hose and calmer pressure and flow behavior) outweigh the decrease in pressure tracking performance (which does not have negative effects for the patient).

VI. Conclusion and Recommendations

The presented controller framework in this paper improves the baseflow tracking in mechanical ventilation. This is achieved by addressing interactions within mechanical ventilation. A control strategy that uses static decoupling combined with factorized Nyquist to design a decentralized controller is presented. To track the baseflow in all phases of breathing, a switching strategy is designed that switches between two flow sensors during a single patient breath. Furthermore, it is experimentally shown that the proposed strategy significantly improves baseflow tracking performance, while only insignificantly decreasing the pressure tracking performance for the selected patient. Concluding, the proposed method indicates that taking interaction into account allows to improves the tracking performance in mechanical ventilation.

A robustness analysis for different patients and spontaneously breathing patients is left for future work. Besides that, a formal stability proof of the switching between controllers is omitted for the sake of brevity.

References

[1] M. A. Warner and B. Patel, *Mechanical Ventilation*, third edit ed. Elsevier Inc., 2013.

[2] H. Wunsch, W. T. Linde-Zwirble, D. C. Angus, M. E. Hartman, E. B. Milbrandt, and J. M. Kahn, "The epidemiology of mechanical ventilation use in the United States," *Critical Care Medicine*, vol. 38, no. 10, pp. 1947–1953, 2010.

[3] M. J. Tobin, *Principle and Practice of Mechanical ventilation*, third edit ed. McGraw-Hill Medical, 2013.

[4] B. Hunnekens, S. Kamps, and N. Van De Wouw, "Variable-Gain Control for Respiratory Systems," *IEEE Transactions on Control Systems Technology*, vol. 28, no. 1, pp. 163–171, 2020.

[5] L. Blanch, A. Villagra, B. Sales, J. Montanya, U. Lucangelo, M. Luján, O. García-Esquirol, E. Chacón, A. Estruga, J. C. Oliva, A. Hernández-Abadia, G. M. Albaiceta, E. Fernández-Mondejar, R. Fernández, J. Lopez-Aguilar, J. Villar, G. Murias, and R. M. Kacmarek, "Asynchronies during mechanical ventilation are associated with mortality," *Intensive Care Medicine*, vol. 41, no. 4, pp. 633–641, 2015.

[6] M. A. Borrello, "Adaptive inverse model control of pressure based ventilation," in *Proceedings of the American Control Conference*, vol. 2. Institute of Electrical and Electronics Engineers Inc., 2001, pp. 1286–1291.

[7] H. Li and W. M. Haddad, "Model predictive control for a multicompartment respiratory system," *IEEE Transactions on Control Systems Technology*, vol. 21, no. 5, pp. 1988–1995, 2013.

[8] J. Reinders, B. Hunnekens, F. Heck, T. Oomen, and N. Van De Wouw, "Adaptive Control for Mechanical Ventilation for Improved Pressure Support," *IEEE Transactions on Control Systems Technology*, vol. 29, no. 1, pp. 180–193, 2021.

[9] M. Scheel, A. Berndt, and O. Simanski, "Iterative learning control: An example for mechanical ventilated patients," *IFAC-PapersOnLine*, vol. 28, no. 20, pp. 523–527, 2015. [Online]. Available: http://dx.doi.org/10.1016/j.ifacol.2015.10.194

[10] A. F. De Castro and L. A. B. Tôrres, "Iterative learning control applied to a recently proposed mechanical ventilator topology," *IFAC-PapersOnLine*, vol. 52, no. 1, pp. 154–159, 2019.

[11] J. Reinders, R. Verkade, B. Hunnekens, N. van de Wouw, and T. Oomen, "Improving mechanical ventilation for patient care through repetitive control," *IFAC-PapersOnLine*, vol. 53, no. 2, pp. 1415–1420, 2020. [Online]. Available: https://doi.org/10.1016/j.ifacol.2020.12.1906

[12] J. Reinders, M. Giaccagli, B. Hunnekens, D. Astolfi, T. Oomen, and N. Van De Wouw, "Repetitive Control for Lur'e-Type Systems: Application to Mechanical Ventilation," *IEEE Transactions on Control Systems Technology*, vol. 31, no. 4, pp. 1819–1829, 2023.

[13] T. Oomen, "Advanced motion control for precision mechatronics: Control, identification, and learning of complex systems," *IEEJ Journal of Industry Applications*, vol. 7, no. 2, pp. 127–140, 2018.

[14] S. Skogestad and I. Postletwaite, *Multivariable Feedback control*. John Wiley and Sons, Ltd, 2006, vol. 01.

[15] J. H. T. Bates, *Lung Mechanics: An inverse modeling approach*. New York: Cambridge University Press, 2009.

[16] E. H. Bristol, "On a new measure of interaction for multivariable process control," *IEEE Transactions on Automatic Control*, vol. 11, no. 1, pp. 133–134, 1966.

[17] P. Grosdidier and M. Morari, "Interaction measures for systems under decentralized control," *Automatica*, vol. 22, no. 3, pp. 309–319, 1986.

[18] G. Zames, "On the input-output stability of time-varying nonlinear feedback systems Part one: Conditions derived using concepts of loop gain, conicity, and positivity," *IEEE Transactions on Automatic Control*, vol. 11, no. 2, pp. 228–238, 1966.

[19] D. Liberzon, *Switching in Systems and Control*. Springer Science+Business Media, LLC, 2003.